Criticality of the nonconservative earthquake model on random spatial networks

Bin-Quan Li and Sheng-Jun Wang*
School of Physics and Information Technology, Shaanxi Normal University, Xi'an 710119, China

(Received 19 September 2017; published 18 July 2018)

We study the nonconservative earthquake model on random spatial networks. The spatial networks are composed of sites on a two-dimensional (2D) plane which are connected locally. Differently from a regular lattice, the locations of sites are modeled in the way that sites are randomly placed on the plane. Using the same connectivity degree as a 2D lattice, however, the spatial network cannot exhibit critical earthquake behavior. Mimicking long range energy transfer, the connection radius is increased and the connectivity degree of the spatial network is increased. Then we show that the model exhibits self-organized criticality. The mechanism of the structural effect is presented. The spatial network includes many modules when connectivity degree is very small. The effect of modular structure on the avalanche dynamics is to limit the spreading of avalanches in the whole network. When the connectivity degree is larger, the long range energy transfer can overcome the effect of local modularity and criticality can be reached.

DOI: 10.1103/PhysRevE.98.012309

I. INTRODUCTION

The concept of self-organized criticality (SOC) was introduced as a possible explanation for the widespread occurrence in nature of long range correlations in space and time [1–5]. Earthquakes are probably the most striking paradigm of SOC that can be observed by humans on earth. According to the empirical Gutenberg-Richter (GR) law [6] the distribution of earthquake events is scale free over many orders of magnitude in energy. The relevance of SOC to earthquakes was first pointed out by Bak and Tang [1] and Sornette and Sornette [7]. According to this theory, plate tectonics provides energy input at a slow timescale into a spatially extended, dissipative system that can exhibit breakdown events via a chain reaction process of propagating instabilities in space and time. The system of driven plates builds up to a critical state with avalanches of all sizes.

Then Olami, Feder, and Christensen (OFC) introduced a nonconservative model on a lattice that displayed SOC [8]. The distribution of avalanche sizes follows a power-law function, and the power-law exponent depends on the dissipation parameter in the OFC model [9]. The OFC model of earthquakes has played an important role in the context of SOC. However, the presence of criticality in the nonconservative version of the OFC model has been controversial since its introduction [9,10] and it is still debated [11–13]. For the presence of criticality, the topology of connections between dynamical units also plays an important role. In the literature, OFC models on different topologies have been investigated.

Lise and Paczuski showed that the critical state is robust over a range of values of the dissipation parameter α [14]. As a structural factor, the boundary condition was considered. They showed that, with both "free" and "open" boundary conditions, the model has the same result of earthquake size distribution that follows a power-law function with the exponent $\tau \simeq 1.8$, completely consistent with the GR law.

To compare with mean-field theory, a random-neighbor (RN) version of the OFC model was proposed. The RN model [15–18] differs from the OFC model only in the choice of neighbors: an unstable site distributes the energy to four randomly chosen sites from the network instead of its nearest neighbors on the lattice. As a result of the change of neighbors, there is criticality only in the conservative case, where it becomes equivalent to a critical branching process.

The OFC model on a quenched random (QR) graph [19] also has been studied. The model represents the correct mean-field limit of OFC model, and can exhibit SOC in the nonconservative regime. The details of the structure properties of the QR graph still have an impact on the appearance of criticality. If all the sites have exactly the same number of nearest neighbors q (both for $q = 4$ and $q = 6$), the dynamics organizes into a subcritical state. In order to observe a power-law distribution of earthquakes, one has to introduce some inhomogeneity. It was shown that it suffices to consider two sites with $q - 1$ neighbors. On the other hand, if sites have different connectivity q_i, there is no criticality.

The effect of small-world and scale-free topologies on the criticality of the nonconservative OFC model has been studied [20–25]. It has been shown that the OFC model on small-world topology exhibited self-organized criticality with a small rewiring probability and undirected connections. In the OFC model on scale-free networks, instead, the strength of disorder does not allow reaching a critical state.

Most works concerning the structural effect have focused on the topological properties of networks [26–37]. However, real systems are often organized in the form of networks where sites and edges are embedded in space. The geometrical properties may provide limits on the organization of networks and have impacts on the dynamics of these networks. In some studies of network dynamics the spatial network has been considered, such as for road networks, power grids, telephone services,

*wangshjun@snnu.edu.cn

and neural networks [38–41]. In these kinds of networks, sites locate over a space with randomness and are connected depending on the distance between each other. All these examples show that topological properties and dynamics of such networks alter with changing space structure. Here it is interesting to study the effect of spatial networks on the OFC model, because randomness is an ineluctable factor in the connection structure between the elements in an earthquake, and the structure is random spatial networks rather than regular lattices.

In this present work, we investigate the critical behavior in a random spatial network in which sites are randomly placed on a plane and are connected locally. By analyzing the distribution of earthquake sizes, we show that the randomness does not allow the network to reach a critical state on sparse networks. However, criticality occurs on a denser network. The mechanism of the disappearance of criticality is presented. We show that sites form modules when networks are sparse, and the avalanche cannot spread as in homogeneous networks. But long range energy transfer overcomes the effect of local modularity, and criticality appears when the network is denser.

II. MODEL

The OFC model is based on the physical earthquake model [42] which consists of blocks coupled by springs and driven by the moving plate. The model is a discrete version of the surface of a moving plate at a homogeneous fault. The OFC model is defined on a two-dimensional square lattice of $L \times L$ sites and each site is associated a real continuous energy E_i. To model the homogeneous scheme, each site is driven continuously and uniformly by the driving block, that is, the value of E_i increases at the same rate. In simulations, one finds the largest value of energy $E_{\max}$ in the system and increases the energy of all sites by the same amount $E_{\text{th}} - E_{\max}$. Therefore the sites with the largest energy reach the threshold value ($E_i \geqslant E_{\text{th}}$) and becomes unstable. As soon as a site becomes unstable, i.e., $E_i \geqslant E_{\text{th}}$, the global driving is stopped and the system evolves according to the following local relaxation rule:

$$\begin{aligned} E_{nn} &\to E_{nn} + \alpha E_i, \\ E_i &\to 0, \end{aligned} \tag{1}$$

where nn stands for the collection of nearest neighbors to node i. The toppling of one site triggers an avalanche, that is, neighbors of this site may become unstable and toppling propagates in the network. The avalanche is over when all of the sites are below E_{th}. Then the driving to all sites recovers. The parameter $\alpha \in [0, 1/4]$ controls the level of conservation of the dynamics, where $\alpha = 1/4$ corresponds to the conservative case, while $\alpha < 1/4$ implies the model is nonconservative. An open boundary condition is used in OFC model.

Here we modify the OFC model by replacing the lattice with a random spatial network. Following the method proposed in Refs. [43–45], the network is built by simple rules:

(a) Randomly pick N sites on a square, whose width is L, such that each site i will have coordinates $0 \leqslant x_i, y_i \leqslant L$, respectively, and $\forall i = 1, 2, ..., N$;

(b) Two sites are connected if the distance between each other is less than the connection radius r_c.

The number of the ith site's neighbors is called the degree of the site and is denoted by k_i. The average degree is defined as $\langle k \rangle = 1/N \sum_i k_i$. For the given values of L and N, the average degree can be changed by tuning the connection radius r_c. Because the degree of sites can be different, the relaxation rule is changed slightly:

$$\begin{aligned} E_{nn} &\to E_{nn} + \frac{\beta}{k_i} E_i, \\ E_i &\to 0. \end{aligned} \tag{2}$$

The parameter β controls the level of conservation of the dynamics and takes values between 0 and 1. It is clear that if $k_i = 4$ and on a two-dimensional lattice the system will become the original OFC model ($\alpha = \beta/4$).

In usual modeling studies, the driving block is rigid and does not change in the process of earthquakes. However, considering the interaction between the site of the driving block, the elastic deformation of the driving block can transfer energy between next nearest neighbors. Therefore, here we consider networks with degrees larger than 4.

According to the rule (2), the energy of an unstable site at the boundary is averagely distributed to each of its nearest neighbors. An alternative boundary condition is that neighbors of one site at the boundary get $\frac{\beta}{\langle k \rangle} E_i$ when the site topples. These two boundary conditions give the same simulation results.

The number of toppling sites during an earthquake is defined as the earthquake size S. In a system of SOC, the distribution of earthquake sizes is a power-law function,

$$P(S) \sim S^{-\tau}. \tag{3}$$

In simulations, we will be concerned with the distribution of avalanche sizes $P(S)$.

III. SIMULATION RESULTS

To compare with the original OFC model, we set the average degree $\langle k \rangle = 4$ in the spatial networks. The network size is $N = 35^2$. In Fig. 1(a), we show the earthquake size distribution $P(S)$ for different values of dissipation parameter β. Different curves result for networks of dissipation parameter $\beta = 0.40$, 0.60, 0.80, 0.90, and 0.95 from left to right. For comparison, the original OFC model with dissipation parameter $\alpha = 0.20$ is also plotted. In the OFC model, the SOC states exhibit that the distribution is a power-law function with an exponential cutoff. The largest avalanche size in the OFC model is about 1000, which is close to the system size N. In the modified OFC model on spatial networks, the distribution of avalanche size depends on the dissipation parameter β, but the distributions obviously diverges from a power-law function. Although the system size is $N = 35^2$, the largest size of avalanche is very small. The distribution only extends to about 100 in the network closest to the conservation case ($\beta = 0.95$). In Fig. 1(b), we use log-linear coordinates to plot the earthquakes size distribution $P(S)$. For different dissipation parameters, the model on spatial networks exhibits that avalanche sizes have an exponential distribution. Therefore, the model on spatial networks does not reach the critical state in a sparse network.

Next, we study the dependence of network states on the parameters of the spatial network. First of all, the effect

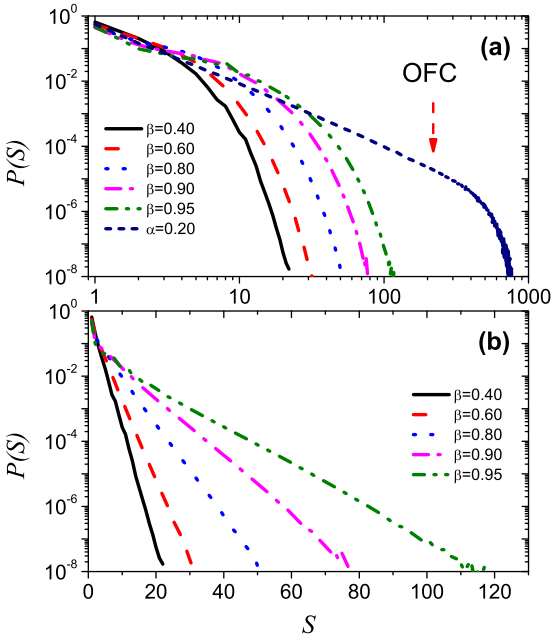

FIG. 1. (a) Distribution of earthquake size. The system has parameters $\langle k\rangle = 4$ and $N = 35^2$ ($r_c = 0.0325$). Different curves correspond to $\beta = 0.40$, 0.60, 0.80, 0.90, and 0.95 from left to right. For comparison, the original OFC model of $\alpha = 0.20$ is shown and is marked by the arrow. (b) Distribution of earthquake size is plotted using log-linear coordinates.

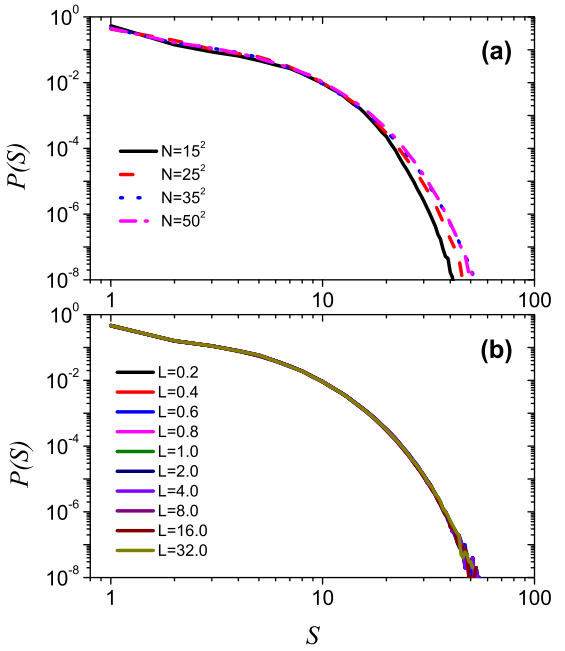

FIG. 2. (a) Distribution of earthquake size for $\langle k\rangle = 4$, $L = 1.0$, and $\beta = 0.80$. Different curves correspond to $N = 15^2$, 25^2, 35^2, and 50^2 ($r_c = 0.079$, 0.046, 0.0325, and 0.0228). (b) Distribution of avalanche sizes for different site density $\rho = N/L^2$. The parameters are $L = 0.2$, 0.4, 0.6, 0.8, 1.0, 2.0, 4.0, 8.0, 16.0, 32.0, $N = 35^2$, $\beta = 0.80$, and $\langle k\rangle = 4$.

of network size is considered. We plot the distribution of earthquake size for systems of different size N. Figure 2(a) shows the simulation results of avalanche size distribution in systems with dissipation parameter $\beta = 0.8$ and network sizes $N = 15^2, 25^2, 35^2$, and 50^2. Although system sizes range from 15^2 to 50^2, the change of the largest size of avalanche is very small.

Besides, the density of sites on the plane is considered. The density is defined as $\rho = N/L^2$. By changing the width L of the plane, the density of sites is varied. At the same time, we adjust the connection radius r_c to keep the average degree fixed. The distribution of avalanche sizes for different densities is shown in Fig. 2(b). The distribution does not change under the adjustment of density.

Furthermore, the long-range energy transfer has been studied in Refs. [46–49]. The spatial network can exhibit this behavior as the system average degree $\langle k\rangle$ increases. In Fig. 3(a), we show the simulation results for systems with different average degree $\langle k\rangle$. Other parameters are $N = 35^2$, $L = 1.0$, and $\beta = 0.90$. One can see that the largest avalanche size tends to N as the average degree increases. The distribution of the original OFC model with dissipation parameter $\alpha = 0.225$ is marked by the arrow in Fig. 3(a). The distribution of systems on spatial networks tends to the distribution of the OFC model as the average degree increases. The left-hand sides of the distribution curves are fitted into power-law functions. For $\langle k\rangle = 144$, the fitted line is shown as the solid line in Fig. 3(a). The slope of the fitted line is $\tau = 1.544$. The slope of the original OFC model of $\alpha = 0.225$ is $\tau = 1.539$. Furthermore, under the high average degree $\langle k\rangle = 288$, we plot the avalanche size distribution for different values of β in Fig. 3(b). We can see that the network exhibits a power-law distribution when the value of β tends to 1. This is similar to the models of RN [15] and small-world networks [20,22].

In simulations, in order to increases the average degree, the connection radius r_c is changed. In a system with $N = 35^2$ and $L = 1.0$, the average degree $\langle k\rangle = 4$ is obtained by using the radius $r_c = 0.0325$, while $\langle k\rangle = 144$ is generated by the radius $r_c = 0.215$. For $\langle k\rangle = 288$, the radius is $r_c = 0.321$. Although the degree changes dramatically, the connection radius is relatively small.

In order to characterize the critical behavior of the model, a finite size scaling (FSS) ansatz is applied [50–53],

$$P_N(S) \sim N^{-\gamma} f\left(\frac{S}{N^D}\right), \tag{4}$$

where f is a suitable scaling function, and γ and D are critical exponents describing the scaling of the distribution function. In Fig. 4, we show the FSS collapse of $P(S)$ for different values of N. As the network size increases, the average degree increases and the ratio $\langle k\rangle/N$ is remained fixed. Different curves correspond to $\langle k\rangle = 36$, $N = 900$, $\langle k\rangle = 72$, $N = 1800$, $\langle k\rangle = 144$, $N = 3600$, and $\langle k\rangle = 288$, $N = 7200$. The distribution $P(S)$ satisfies the FSS hypothesis well except at the stage of crossover, like the results in [14]. The critical exponents derived from the fit of Fig. 4 are $\gamma = 0.6714$ and $D = 0.436$, and the slope of the straight line is $\tau = 1.5$. The FSS hypothesis implies that, for asymptotically large N, $P_N(S) \sim S^{-\tau}$ and the value of the exponent is $\tau = \gamma/D \simeq 1.54$. Because of the numerical uncertainty on the estimate, it is difficult to assert

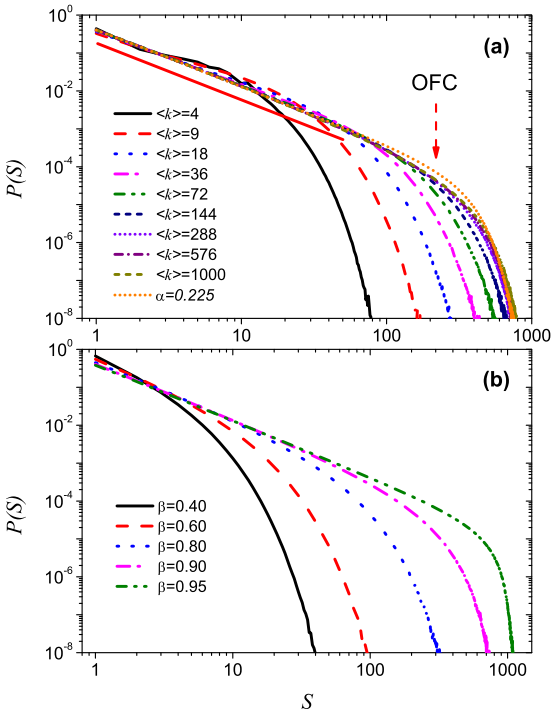

FIG. 3. (a) Distribution of earthquake size for different average degree $\langle k\rangle$ with $N = 35^2$, $L = 1.0$, $\beta = 0.90$. Different curves correspond to $\langle k\rangle = 4$, 9, 18, 36, 72, 144, 288, 576, and 1000 from left to right. (b) Distribution of earthquake size for different values of β with $N = 35^2$, $L = 1.0$, $\langle k\rangle = 288$. Different curves correspond to $\beta = 0.40$, 0.60, 0.80, 0.90, and 0.95 from left to right. The original OFC model of $\alpha = 0.225$ is shown and is marked by the arrow. The fitted curve is shown as red solid line.

with certainty that τ is a novel exponent different from the one for the conservative RN model ($\tau \simeq 1.5$).

We give an interpretation of the effect of connectivity degree of networks on the network states. When networks are sparse, the networks may divide into small clusters. In Fig. 5, we plot the number of clusters in a network with $N = 35^2$

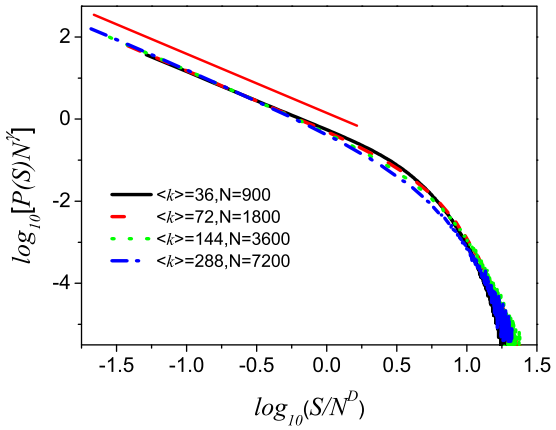

FIG. 4. Finite-size scaling plots of $P(S)$ in systems for different values of the system size N. The parameters are $\beta = 0.90$, $L = 1.0$. Different curves correspond to $\langle k\rangle = 36$, $N = 900$, $\langle k\rangle = 72$, $N = 1800$, $\langle k\rangle = 144$, $N = 3600$, and $\langle k\rangle = 288$, $N = 7200$.

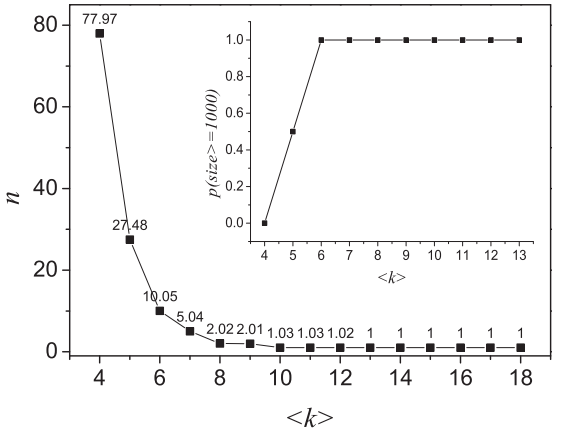

FIG. 5. The number of clusters in a spatial network with $N = 35^2$ versus the average degree $\langle k\rangle$. Data points are averaged over 100 realizations. Inset: probability that the network has a giant cluster which includes most of the sites.

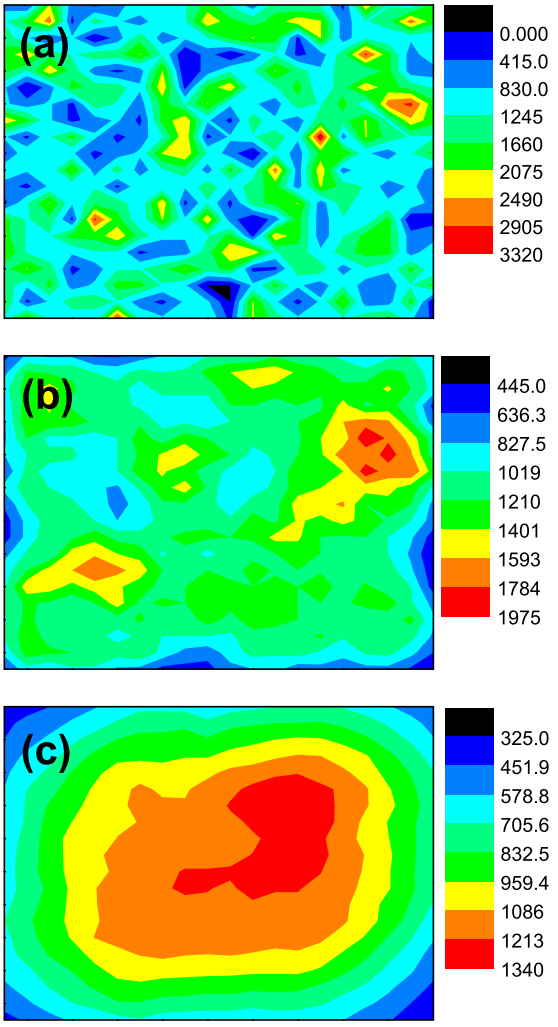

FIG. 6. Density of sites, which is computed in a circle with radius r_c. Parameters are $N = 35^2$, (a) $\langle k\rangle = 4$ ($r_c = 0.0325$), (b) $\langle k\rangle = 36$ ($r_c = 0.10$), and (c) $\langle k\rangle = 288$ ($r_c = 0.32$).

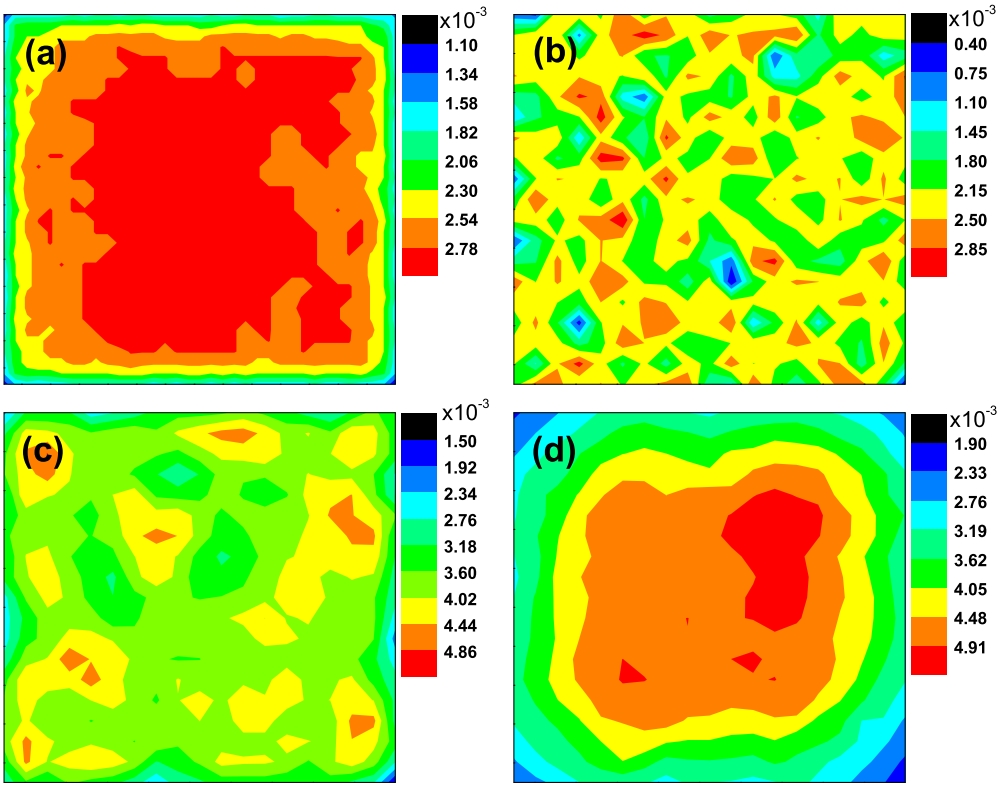

FIG. 7. Probability of a site participating in an avalanche. (a) The original OFC model with $N = 35^2$ and $\alpha = 0.20$. (b) Spatial network with $\langle k \rangle = 4$. (c) Spatial network with $\langle k \rangle = 36$. (d) Spatial network with $\langle k \rangle = 288$. Other parameters are $N = 35^2$ and $\beta = 0.80$. The probability is computed using 10000 earthquakes.

sites and different average degree $\langle k \rangle$. The result is averaged over 100 realizations. When the average degree $\langle k \rangle = 4$, there are 78 isolated clusters in the network. Clusters appear at the place where the density of sites is higher. The connection is too sparse in the spatial network, and sites in the 2D plane are not connected. Therefore, the avalanche cannot spread to the whole system.

As the average degree increases, the small clusters are connected together to form larger clusters. At $\langle k \rangle = 6$ a giant cluster is formed. Although the giant cluster includes almost all sites in the system, SOC cannot be reached. Similarly, at $\langle k \rangle = 13$ all sites are connected, but SOC cannot be reached. A connected network does not suffice to reach criticality in the OFC model on spatial networks. In fact, the criticality is hindered by the modular structure which has dense intramodule connections and sparse intermodule connections. It is shown that the effect of modular structure on the avalanche dynamics is to limit the spreading of avalanches between modules and prevent the model from becoming critical [48,54,55].

To illustrate the modular structure feature, we compute the local density of sites. For a position on the plane, we consider the neighborhood as a circle with radius r_c, which is the connection radius used in generating the spatial network. The local density is the ratio of the site number in a circle over the area of the circle, $\varrho = n_i/(\pi * r_c^2)$. Figure 6 shows the local density of sites for different values of $\langle k \rangle$ (or r_c), in a network with size $N = 35^2$. It can be seen that the model with larger $\langle k \rangle$ possesses more homogeneous local density.

In order to confirm the effect of modular structure on the avalanche dynamics, we calculate the probability of a site participating in each avalanche. For the original OFC model with the parameters $N = 35^2$ and $\alpha = 0.20$, the probability is shown in Fig. 7(a). The number of avalanche used in estimating the probability is 10000. It can be seen that the probability of a site participating in an avalanche in the original OFC model is homogeneous, as shown in Fig. 7(a). This means that avalanches propagate randomly without preference in the OFC model. In the spatial network model, we divide the plane into 20^2 regions. For each region, the probability of sites participating in an avalanche is computed. For a network with average degree $\langle k \rangle = 4$, the probability is shown in Fig. 7(b). The probability exhibits the feature of the local density of sites. The probabilities for larger values of $\langle k \rangle$ are shown in Figs. 7(c) and 7(d). It can be seen that as the average degree $\langle k \rangle$ becomes larger, the probability becomes more homogeneous and similar to the results of the original OFC model.

These numerical results about structural features reveal that the effect of modular structure on the avalanche dynamics is to hinder the avalanche spreading over the whole network and to prevent the model from reaching a critical state. But long range energy transfer overcomes the effect of local modularity. Criticality is reached when the network is denser.

IV. CONCLUSION

We have studied the nonconservative earthquake model on spatial networks. The spatial network is similar to as lattice

as sites are distributed in space and are connected locally. However, spatial networks include randomness in the way that sites are randomly placed on a 2D plane. We are concerned with the effect of the randomness on criticality in earthquakes.

We made an extensive numerical study of the earthquake model on random spatial networks. We showed that there is not SOC on sparse spatial networks; for example, on networks which have the same connectivity degree as a regular square lattice. However, this model on spatial networks exhibits SOC when the average degree is large and the system tends to conservation.

We presented the mechanism of the structural effect on SOC by numerical investigation. When the average degree is very small, spatial networks include many modules which are formed due to the fluctuation of spatial density of sites on the plane. The modular structure hinders the spreading of avalanches in the whole network. Connection degree is increased as connection radius increases. Larger connection radius enables energy transfer over a long range. The long range energy transfer overcomes the effect of local modularity and SOC can be reached. These results may provide new insight into the self-organized criticality in earthquakes.

ACKNOWLEDGMENTS

This work was supported by NSFC (Grants No. 11675096 and No. 11305098), the Fundamental Research Funds for the Central Universities (Grant No. GK201702001), and Interdisciplinary Incubation Project of SNNU (Grant No. 5).

[1] P. Bak, C. Tang, and K. Wiesenfeld, Phys. Rev. Lett. **59**, 381 (1987).
[2] H. J. Jensen, *Self-Organised Criticality* (Cambridge University Press, Cambridge, 1998).
[3] C. Haldeman and J. M. Beggs, Phys. Rev. Lett. **94**, 058101 (2005).
[4] O. Kinouchi and M. Copelli, Nat. Phys. **2**, 348 (2006).
[5] S.-J. Wang, G. Ouyang, J. Guang, M. Zhang, K. Y. M. Wong, and C. Zhou, Phys. Rev. Lett. **116**, 018101 (2016).
[6] B. Gutenberg and C. F. Richter, Ann. Geophys. **9**, 1 (1956).
[7] A. Sornette and D. Sornette, Europhys. Lett. **9**, 197 (1989).
[8] Z. Olami, H. J. S. Feder, and K. Christensen, Phys. Rev. Lett. **68**, 1244 (1992).
[9] W. Klein and J. Rundle, Phys. Rev. Lett. **71**, 1288 (1993).
[10] K. Christensen, Phys. Rev. Lett. **71**, 1289 (1993).
[11] J. X. de Carvalho and C. P. C. Prado, Phys. Rev. Lett. **84**, 4006 (2000).
[12] J. X. de Carvalho and P. C. Prado, Phys. Rev. Lett. **87**, 039802 (2001).
[13] K. Christensen, D. Hamon, H. J. Jensen, and S. Lise, Phys. Rev. Lett. **87**, 039801 (2001).
[14] S. Lise and M. Paczuski, Phys. Rev. E **63**, 036111 (2001).
[15] S. Lise and H. J. Jensen, Phys. Rev. Lett. **76**, 2326 (1996).
[16] M.-L. Chabanol and V. Hakim, Phys. Rev. E **56**, R2343 (1997).
[17] H.-M. Broker and P. Grassberger, Phys. Rev. E **56**, 3944 (1997).
[18] O. Kinouchi, S. T. R. Pinho, and C. P. C. Prado, Phys. Rev. E **58**, 3997 (1998).
[19] S. Lise and M. Paczuski, Phys. Rev. Lett. **88**, 228301 (2002).
[20] F. Caruso, V. Latora, A. Pluchino, A. Rapisarda, and B. Tadic, Eur. Phys. J. B **50**, 243 (2006).
[21] F. Caruso, V. Latora, and A. Rapisarda, *Complexity, Metastability and Nonextensivity* (World Scientific, Singapore, 2005), pp. 355–360.
[22] L. De Arcangelis and H. J. Herrmann, Physica A (Amsterdam) **308**, 545 (2002).
[23] A. F. Rozenfeld, R. Cohen, D. ben-Avraham, and S. Havlin, Phys. Rev. Lett. **89**, 218701 (2002).
[24] M. Lin, X.-W. Zhao, and T.-L. Chen, Commun. Theor. Phys. **41**, 557 (2004).
[25] M. Lin, X.-W. Zhao, and T.-L. Chen, Commun. Theor. Phys. **46**, 1011 (2006).
[26] P. Rattana, L. Berthouze, and I. Z. Kiss, Phys. Rev. E **90**, 052806 (2014).
[27] L. Liucci, L. Melelli, C. Suteanu, and F. Ponziani, Geomorphology **290**, 236 (2017).
[28] D. Markovic and C. Gros, Phys. Rep. **536**, 41 (2014).
[29] C. A. Serino, W. Klein, and J. B. Rundle, Phys. Rev. E **81**, 016105 (2010).
[30] A. Allen-Perkins, J. Galeano, and J. M. Pastor, Phys. Rev. E **94**, 052304 (2016).
[31] O. M. Braun and M. Peyrard, Phys. Rev. E **87**, 032808 (2013).
[32] O. M. Braun and E. Tosatti, Phys. Rev. E **90**, 032403 (2014).
[33] L. de Arcangelis, C. Godano, J. R. Grasso, and E. Lippiello, Phys. Rep. **628**, 1 (2016).
[34] L. Zhou and S.-J. Wang, Fractals **26**, 1850038 (2018).
[35] H. Hoffmann, Phys. Rev. E **97**, 022313 (2018).
[36] S. V. Mykulyak, Phys. Rev. E **97**, 062130 (2018).
[37] B.-Q. Li and S.-J. Wang, Commun. Theor. Phys. **69**, 280 (2018).
[38] S. Hergarten and H. J. Neugebauer, Phys. Rev. Lett. **86**, 2689 (2001).
[39] M. Kaiser and C. C. Hilgetag, Phys. Rev. E **69**, 036103 (2004).
[40] M. C. Gonzalez, P. G. Lind, and H. J. Herrmann, Phys. Rev. Lett. **96**, 088702 (2006).
[41] G. Bagler, Physica A (Amsterdam) **387**, 2972 (2008).
[42] R. Burridge and L. Knopoff, Bull. Seismol. Soc. Am. **57**, 341 (1967).
[43] M. Barthelemy, Phys. Rep. **499**, 1 (2011).
[44] J. Dall and M. Christensen, Phys. Rev. E **66**, 016121 (2002).
[45] G. Nemeth and G. Vattay, Phys. Rev. E **67**, 036110 (2003).
[46] R. Dominguez, K. F. Tiampo, C. A. Serino, and W. Klein, Phys. Rev. E **87**, 022809 (2013).
[47] Z.-G. Huang, S.-J. Wang, X.-J. Xu, J.-T. Sun, and Y.-H. Wang, J. Stat. Mech. (2009) P09005.

[48] S.-J. Wang and C. Zhou, New J. Phys. **14**, 023005 (2012).
[49] S. Stein Ross, Nature (London) **402**, 605 (1999).
[50] P. Grassberger, Phys. Rev. E **49**, 2436 (1994).
[51] L. P. Kadanoff, S. R. Nagel, L. Wu, and S. M. Zhou, Phys. Rev. A **39**, 6524 (1989).
[52] K. Christensen and Z. Olami, Phys. Rev. A **46**, 1829 (1992).
[53] F. P. Landes and E. Lippiello, Phys. Rev. E **93**, 051001 (2016).
[54] M. Zhao, C. Zhou, Y. Chen, B. Hu, and B.-H. Wang, Phys. Rev. E **82**, 046225 (2010).
[55] M. Kaiser, M. Gorner, and C. C. Hilgetag, New J. Phys. **9**, 110 (2007).